Chemical Engineering Journal 95 (2003) 171–177

Chemical Engineering Journal

www.elsevier.com/locate/cej

Trajectories of charged drops in a liquid–liquid system

A.P. Hume [a], L.R. Weatherley [a], J. Petera [b,*]

[a] *Department of Chemical and Process Engineering, University of Canterbury, Christchurch, New Zealand*

[b] *Faculty of Environmental and Process Engineering, The Technical University of Lodz, ul. Wolczanska 175, Lodz 90-924, Poland*

Abstract

The enhancement of liquid droplet dispersion and motion in liquid–liquid contactors by the introduction of electrostatic charge and an electric field is a potentially important method of process intensification for solvent extraction and other liquid–liquid operations. An understanding of those factors which influence drop motion in these systems is essential for the prediction of hydraulic and mass transfer data which in turn are necessary for the design of commercial scale equipment. The work described here aims to develop an accurate method of measuring and predicting single drop trajectories in electrically charged liquid–liquid systems. Two experimental methods are described, including a simple video recording system in which the trajectories of drops were manually digitised and a more elegant procedure in which space-time images of moving droplets were analysed using image analysis software. Three liquid–liquid systems were studied: pre-saturated sunflower oil/water, pre-saturated 1-decanol/water and pre-saturated silicone oil/water. The trajectories were determined at a range of applied electrical field strengths and over a range of drop sizes and in two scales of experimental geometry. The results were compared in each case with the trajectories predicted using a quantitative finite-element model and good agreement was obtained.

Keywords: Charged drops; Liquid–liquid system; Extraction; Finite element model

1. Introduction

The importance of droplet behaviour in determining the performance of liquid–liquid extraction equipment is very well known [1]. The size and hold-up of the droplet phase have a profound influence on the mass transfer rate in continuous contactors, and also dictate the hydraulic requirements of the contactor for the efficient handing of both dispersed and continuous phase throughputs. The size distribution of drops and the dynamic (as opposed to the static) dispersed phase hold-up directly affect the interfacial area per unit volume available for mass transfer. Another significant factor is the frequency at which drops coalescence and break-up during their passage through the contactor. A high frequency of break-up/coalescence/break-up generally enhances mass transfer due to the macro-disturbances which are imparted to the liquid phase comprising the interior of each drop. The frequency of drop break-up and coalescence may also affect the effective size distribution of drops within the contactor and thus the interfacial area. A further factor which affects mass transfer rate is the linear velocity of the drop phase relative to the continuous phase, since the higher the velocity, the higher the interfacial shear rate. This will enhance the mass transfer rate in the continuous phase surrounding the drop. Another important factor affecting the overall performance of the contactor is the degree of mixing (and backmixing) present in the continuous phase, and the extent to which macro-scale backmixing and forward mixing of individual drops occurs during their passage through the contactor. In this respect, the residence time distributions of the drops and of the continuous phase are of some significance as in continuous chemical reactor systems [2].

In this paper, however, we are not concerned with swarms of droplets where such effects with regard to the continuous phase would be important, but rather with single drops in unhindered motion. Specifically the main interest is the study of the movement of electrically charged drops in a column contactor, since placement of an electrostatic charge on drops in a liquid–liquid systems and the subsequent enhancement of their motion using an externally applied electrical field can improve mass transfer rate. Such improvements have been reported over many years by a number of workers [3,4]. Observations have been reported of mass transfer enhancement in a range of liquid–liquid systems and in range of contactor geometries. However, none of these studies attempt to discover the individual mechanisms responsible for the observed enhancements in mass transfer based on an understanding of the mechanics of charged drop motion.

Previous work by Petera et al. [5] focused on the measurement and prediction of the motion of charged spherical ion-exchange beads through a non-conducting liquid across which a high-voltage field was maintained. The theoretical

* Corresponding author. Fax: +48-42-636-56-63.

1385-8947/$ – see front matter © 2003 Published by Elsevier Science B.V.
doi:10.1016/S1385-8947(03)00101-3

approach adopted was based upon the fundamental relationships governing the electrical field, the potential distribution, and the equations of motion. Of particular relevance to the current research was the successful development of an algorithm to calculate the space charge distribution in the continuous phase liquid, subsequent to the application of the external electrical field.

The problem of charge drop motion in a liquid–liquid system is more complex than in the case of rigid spheres, since the drops experience time-dependent deformation and unsteady internal flows during their passage through the continuous phase, which in turn gives rise to changes in motion. Bozzi et al. [6] showed that the motion of uncharged drops in a liquid–liquid system could be accurately determined by solution of the Navier–Stokes equations applied to each phase. They considered the steady axisymmetric flow in and around a deformable drop moving under the influence of gravity along the axis of a vertical tube at intermediate Reynolds number by solving the non-linear free-boundary problem using a Galerkin finite-element method. Bozzi et al. [6] considered the motion of deformable droplets (albeit uncharged) but only along the axis of symmetry and such an approach is insufficient for trajectory prediction. By contrast, Petera et al. [5] adopted a more rigorous approach, albeit for the motion of solid spheres, in which the complex hydrodynamics in the vicinity of the interface were simplified using a drag coefficient relationship. Satisfactory experimental validation of this approach, which also took into account the effects of an externally applied electric field, was clearly demonstrated for two-dimensional trajectories.

A further consideration is the development of this approach to calculation of mass transfer rate. Petera and Weatherley [7] showed that mass transfer from single unhindered falling drops could be predicted with reasonable accuracy, by solving the equations of motion for each drop and by incorporation of the Stefan–Maxwell equations into the calculation scheme.

The work described in this paper therefore examined the further case of charged liquid drop motion. The scope of the work was the experimental recording of charged drop three-dimensional trajectories in a liquid–liquid system in the presence of an externally applied field. A number of variables were studied including applied field strength, flowrate, physical properties of the liquid, and contactor geometry. The measured trajectories are compared with the theoretical predictions, but the scope of this paper is introductory and is limited to sample comparisons for the two-dimensional case only. A more comprehensive consideration of the two-dimensional and the three-dimensional case will be included in later papers.

2. Theoretical

A summary of the theoretical approach is given here and full details are published elsewhere [5]. The electric field in the domain is described by the well-known Poisson differential equation:

$$\nabla \cdot (\varepsilon_r \nabla \Phi) = -\frac{\sigma}{\varepsilon_0} \tag{1}$$

where Φ is the electrical potential, ε_r the relative permittivity, ε_0 the dielectric constant of free space and σ is the charge density.

The space charge distribution was obtained by using the transport equation to simulate the migration of space charge entities in the continuum between the electrodes:

$$\frac{\partial \sigma}{\partial t} + \underline{u} \cdot \nabla \sigma = 0 \tag{2}$$

where t is the time and $\underline{u}$ is the velocity field of the migration σ is determined from the mobility α and the local field strength E, according to the relationship:

$$\underline{u} = \alpha \cdot E \tag{3}$$

The field strength is related to the electrical potential by the equation:

$$E = -\nabla \Phi \tag{4}$$

The solution of the equations to yield the space charge distribution, and the electric field is fully described by Petera et al. [5]. This was by numerical discretization of the equations, using the Galerkin discretization procedure for the calculation of the electrical field, and using the Lagrangian numerical framework for the calculation of space charge distribution. The resultant field distribution was obtained by iterative solution of Eqs. (1)–(3). Thus, the overall electrical field through which the drop motion occurs is obtained by superposition of the externally applied electrical field and the field due to the space charge.

The final stage of the model involves the setting up and solution of the equations of motion for a single charged drop moving through the continuous phase, under the influence of the resultant electrical field E. The calculation of trajectory is based on the following forces which act on the drop.

Electrical force:

$$E_E = E \cdot q \tag{5}$$

where q is the electric charge of the particle, and it may change according to the very well known rule (for constant permittivity ε_r and conductivity κ of the liquid):

$$q = q_0 \exp\left(-\frac{t}{\lambda}\right) \tag{6}$$

where $\lambda = \varepsilon_0 \varepsilon_r / \kappa$ is the relaxation time of the dielectric liquid.

Drag force:

$$E_D = \frac{\pi \mu_c d (2\mu_c + 3\mu_d)}{\mu_c + \mu_d} \underline{v} \tag{7}$$

where μ_c and μ_d are the viscosities of the continuous and dispersed phases respectively, d is the drop diameter and $\underline{v}$ the velocity.

Buoyancy force:

$$E_B = \tfrac{1}{6}\pi d^3(\rho_d - \rho_c)\underline{g} \quad (8)$$

where ρ_d and ρ_c are the respective densities of the drop phase and the continuous phase, $\underline{g}$ is the gravity vector (0, −9.81, 0).

Inertial force:

$$E_I = \frac{1}{6}\pi d^3 \rho_d \frac{d\underline{v}}{dt} \quad (9)$$

Thus, the dynamical equation can be written as follows:

$$\frac{d\underline{v}}{dt} = A_1 E_q + A_2 \underline{v} + A_3 \underline{g} \quad (10)$$

where

$$A_1 = \frac{6}{\pi d^3 \rho_d}, \quad A_2 = \frac{6\mu}{d^2 \rho_d}\left(\frac{2\mu_c + 3\mu_d}{\mu_c + \mu_d}\right),$$
$$A_3 = 1 - \frac{\rho_c}{\rho_d} \quad (11)$$

Eq. (9) is solved numerically together with obvious definition of the particle velocity:

$$\underline{v} = \frac{d\underline{x}}{dt} \quad (12)$$

where $\underline{x}$ is the position vector, in order to determine the droplet trajectory in the domain with the electric field determined using the numerical procedure.

3. Experimental

3.1. Apparatus

The droplet trajectory experiments were carried out in one of two columns each fabricated with a PVC base and glass walls. The columns were equipped with a charged, partially insulated stainless steel electrode located near to the bottom of the column, protruding horizontally into the centre of the column. Each column was fitted with a PVC lid through which was located a protruding earthed, partially insulated stainless steel electrode. This also acted as a nozzle for the injection of the dispersed phase liquid into the continuous phase liquid. A sketch of the column design, showing the basic shape and arrangement is shown in Fig. 1. The dimensions used for each set of experiments are indicated in Table 1.

Prior to each experiment the walls of the column were silanised with a 2% solution of dichlorodimethylsilane in 1,1,1-trichloroethane, i.e. a hydrophobic coating was applied to the inside of the glass walls. This prevented charged droplets from being attracted to and clinging to the glass walls. The columns were thoroughly cleaned and rinsed with distilled water prior to filling with the selected continuous phase. Three continuous phase liquids were used, sunflower oil, *n*-decanol, and silicone oil. In each case, the liquid was pre-saturated with de-ionised water in order to prevent any minor mass transfer of water during the trajectory experiments.

The electrical field was applied to the contactor by means of a high dc voltage source (Brandenburg, Models 2507, 2878N, 828P) which was connected directly to the contactor electrode. The voltage was measured using a high-voltage digital voltmeter (Brandenburg, Model 139D). The temperature of the column was monitored using a digital thermometer (Fluke 52). Convective cooling was applied to the exterior of the contactor by means of an electric fan to prevent incidental heating of the contactor from the close proximity illumination and arising from any minor Coulombic heating effects within the contactor. No significant changes in temperature were recorded. Prior to the trajectory measurements the external field was applied for a period of 3 h to allow space charge migration to occur and the attainment of space charge equilibrium. Earlier trials [8] showed that space charge migration equilibrium was typically achieved in a contactor of similar geometry within 30 min. The dispersed phase was injected into the continuous phase through the earthed nozzle at constant rate, using a syringe pump (Perfusor VI).

The droplet trajectories were filmed using a Sony Handycam video camera (25 frames/s). The camera was located approximately 3 m from the column in order to minimise parallax error. A mirror was mounted adjacent to the column at a 45° angle to the wall in order that the drop trajectories could be reviewed and recorded in three dimensions. The column was illuminated reflectively using spotlights and a white reflector board.

Relevant physical property data for each system were measured independently using established techniques which are described in detail by Hume [9]. These comprised: density, viscosity, interfacial tension, and dielectric constant. The relevant measurements are summarised in Tables 2 and 3 for the dispersed phase and continuous phases respectively. Literature values for water were used in the case of the dispersed phase.

3.2. Calculation of the trajectory results

The droplet trajectories were converted from video form to digital (x, y, z, t) form, using one of two methods. A

Table 1
Geometric data for the contactor (Fig. 1)

Geometry	*B* (mm)	*D* (mm)	*E* (mm)	*I* (mm)	ID (mm)	OD (mm)	*S* (mm)
A	10	10	4.3	70	2.3	3.23	50
B	20	10	5.02	142	4.48	6.45	100

Table 2
Physical property data—dispersed phase

Property	Relationship/value used
Density (kg m^{-3})	995 ± 0.7
Viscosity (Pa s) (T in K)	$\ln(\mu_w) = -12.37 + \frac{1313.78}{-53.19 + T}$

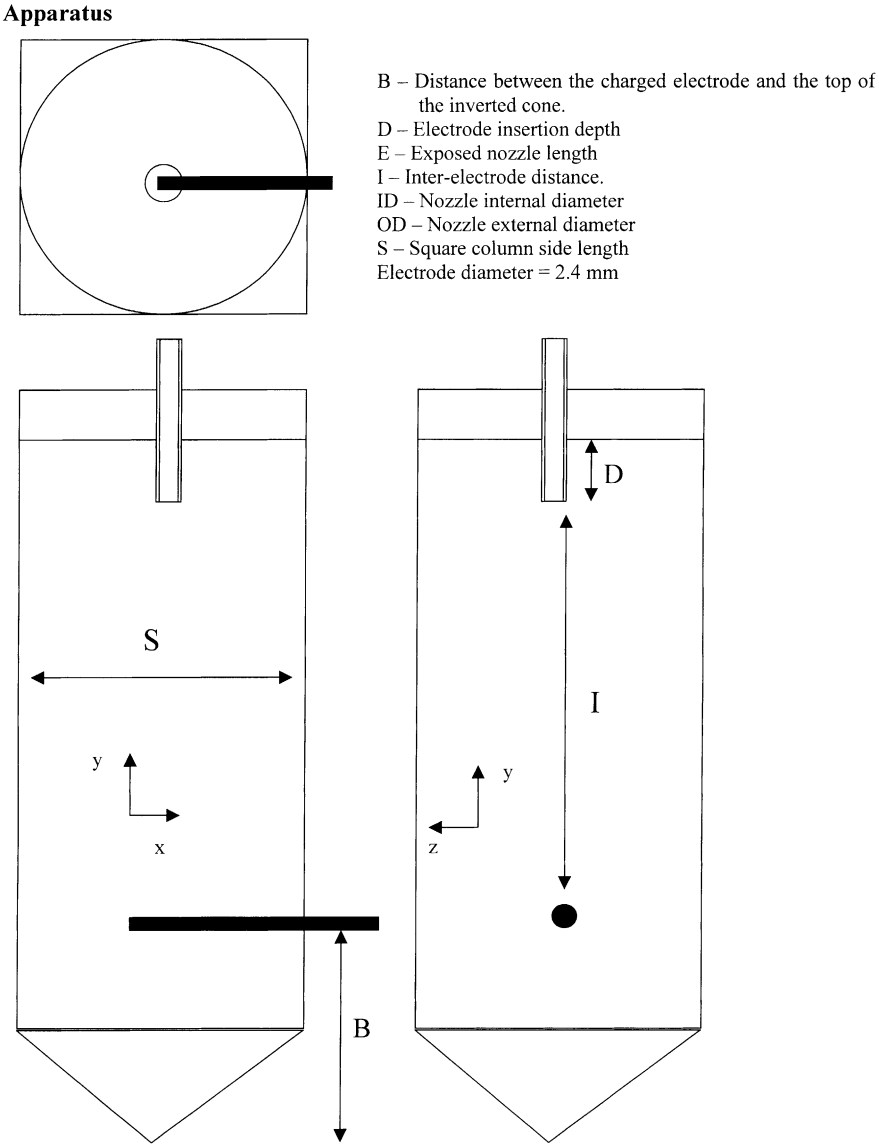

Fig. 1. Layout and essential dimensions of the contactor.

number of the data were initially manually transposed directly from the television monitor screen onto a pair of transparent sheets, for the front-on and side-on (mirror) images respectively. The droplet trajectories were tracked frame by frame by placing small dots onto the sheets to represent the position of each drop in successive time frames. The numerical co-ordinate values for each successive drop position were then obtained by overlaying the transparent sheet onto scaled graph paper and co-ordinate—time values read accordingly. The trajectories of each of the drop were averaged to obtain a final trajectory.

A second method involved the use of image analysis software (Optimus version 6.5). This was found to be particularly valuable in cases where the droplet size distribution was non-uniform and when droplet coalescence occurred. These cases involved the tracking of individual droplet trajectories, which could not be averaged because they differed between droplets. The video images of the droplet trajectories being studied were imported frame by frame into the computer. The co-ordinates of every drop in every frame were then found using the "point morphometry" function of the package.

All droplet trajectories were determined relative to the centre of the tip of the earthed nozzle, which was taken as the origin, with three-dimensional co-ordinates $(x, y, z) = (0, 0, 0)$. The three-dimensional co-ordinates of each droplet were taken from the centre of the droplet in all cases.

Average droplet sizes were determined from the known dispersed phase flowrate and the average time between the detachments of the droplets. In the case of small drops, the use of the image analysis software again was useful for the determination of mean drop size.

Table 3
Physical property data—continuous phase

Property	Relationship/value used
Density ($kg\,m^{-3}$) (T in °C)	$\rho_{n\text{-decanol}} = 7.1151 \times 10^{-4}T^2 - 0.7321T + 847.99$
	$\rho_{\text{sunflower oil}} = -3.3444 \times 10^{-5}T^2 - 0.6824T + 934.03$
	$\rho_{\text{silicone oil}} = 2.09 \times 10^{-4}T^2 - 0.90806T + 982.44$
Viscosity (Pa s) (T in K)	$\mu_{n\text{-decanol}} = \exp\left[\frac{3287.7}{T} - 15.438\right]$
	$\mu_{\text{sunflower oil}} = \exp\left[\frac{3343.5}{T} - 14.167\right]$
	$\mu_{\text{silicone oil}} = \exp\left[\frac{1712.2}{T} - 8.7283\right]$
Interfacial tension ($dyn\,cm^{-1}$) (T in °C)	$\gamma_{n\text{-decanol}} = 1.7061 \times 10^{-6}T^4 - 2.5753 \times 10^{-4}T^3 + 1.2174 \times 10^{-2}T^2 - 0.141502T + 8.4792$
	$\gamma_{\text{sunflower oil}} = -1.29502 \times 10^{-5}T^3 + 1.6147 \times 10^{-2}T^2 - 0.102139T + 35.87$
	$\gamma_{\text{silicone oil}} = 30.5$
Dielectric constant	n-Decanol: 6.3 Sunflower oil: 3.11 silicone oil: 2.63

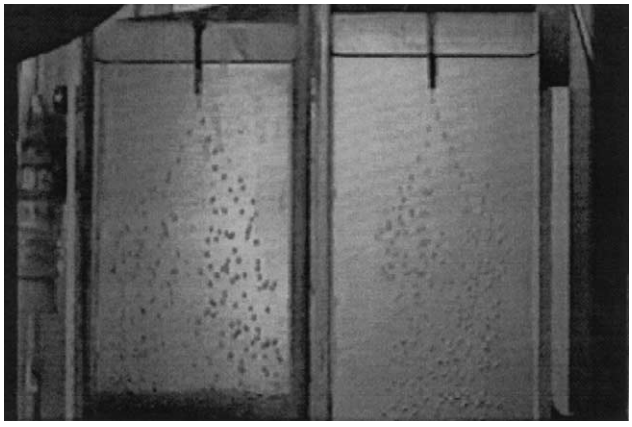

Fig. 2. Video frame of trajectory experiment.

An example of a video image of the contactor during operation is shown in Fig. 2 and the drops are clearly visible. The figure comprises two side by side images which correspond to simultaneous shots taken at identical time at 90° to each other.

4. Discussion of results

Fig. 3 shows the space charge map for the computational domain subsequently used for the modelling of the trajectory behaviour. The non-uniform distribution of the space charge is very apparent. As expected the predictions show the concentration of space charge in the vicinity of the electrodes with significant differences between the lower (charged) electrode and the nozzle (earthed). The calculated distribution is consistent with that calculated and used successfully in earlier work [5] involving a different system and a cylindrical geometry.

The electrical potential contours are shown in Fig. 4 and these also reflect the non-uniform nature of the electrical environment in which the drops are moving.

Figs. 5–7 show the comparison between the experimental and simulated droplet trajectories for water drops moving through sunflower oil, 1-decanol, and silicone oil, respectively. In the case of the sunflower oil, experiments were conducted at an electrode voltage applied voltage of −7.50 kV and in the larger of the two contactor geometries (geometry A, Table 1). Under these conditions, the best fit trajectory was obtained using a relaxation time of 3.0 s which is consistent with the known electrical properties of the oil. An approximate value of conductivity was estimated

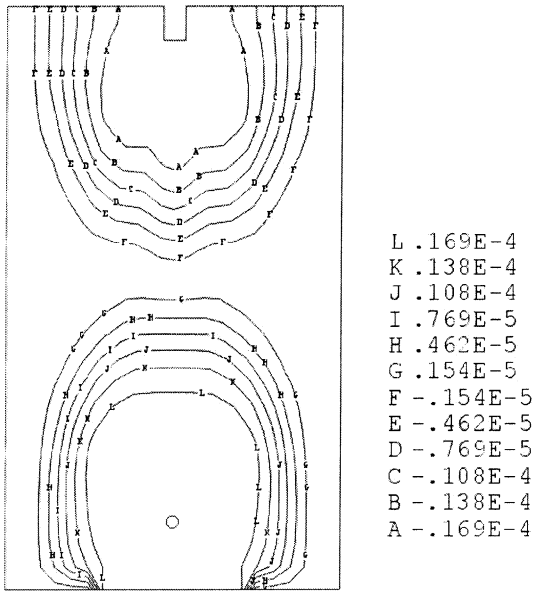

Fig. 3. The calculated space charge distribution map.

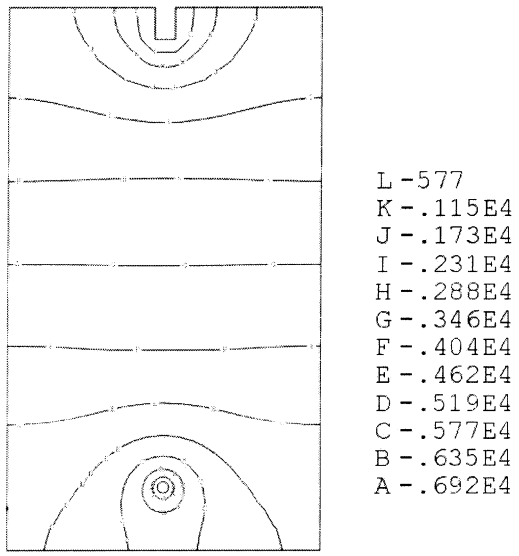

Fig. 4. The calculated electrical field map.

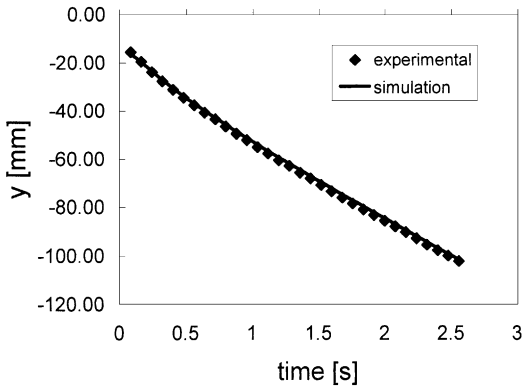

Fig. 5. One-dimensional droplet trajectory for sunflower oil: external field = −7.50 kV, dispersed phase flowrate = 320 ml h^{-1}, geometry B.

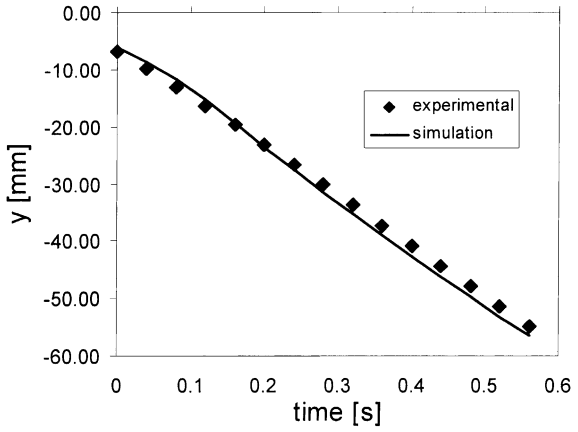

Fig. 6. One-dimensional droplet trajectory for *n*-decanol: external field = +1.50 kV, dispersed phase flowrate = 320 ml h^{-1}, geometry A.

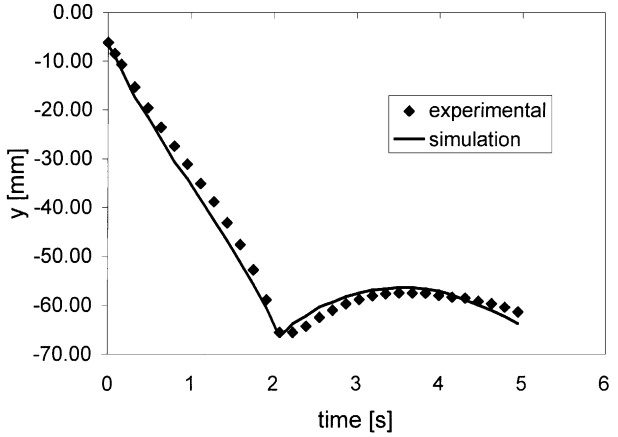

Fig. 7. One-dimensional droplet trajectory for water drops in silicone oil: external field = 6.00 kV, dispersed phase flowrate = 65 ml h^{-1}, geometry A.

for sunflower oil. Using the formula for relaxation time ($\tau = \varepsilon\varepsilon_0/K$) and the experimentally determined value of the dielectric constant of sunflower oil ($\varepsilon = 3.11$), the conductivity (K) is found to be 1.4×10^{-11} S m^{-1}.

Although it would have been preferable to calculate the relaxation time directly from the conductivity and dielectric constant, this was difficult to achieve in practice due to the difficulty of measuring the conductivity of such weakly conducting liquids let alone any fluctuations in these and the lack of literature values.

The comparison of predicted trajectory against measured for *n*-decanol. Fig. 6 is slightly less satisfactory than for sunflower oil. Of particular importance in the *n*-decanol system is that the relaxation time was very small, meaning that electrical forces were very small and that droplet motion was predominantly governed by buoyancy and drag forces. The low interfacial tension of the *n*-decanol/water system also meant that the electrostatic spraying regime was reached at very low voltages. The relaxation time value used in the *n*-decanol simulation was 0.35 s. However, using the formula for relaxation time ($\tau = \varepsilon\varepsilon_0/K$), the experimentally determined value of the dielectric constant of *n*-decanol; $\varepsilon = 6.3$, and a literature value [8] of the conductivity of *n*-decanol; $K = 2.11 \times 10^{-7}$ S m^{-1}, the calculated relaxation time is 2.6×10^{-4} s. Therefore, the relaxation time used in the simulations for the *n*-decanol experiments may be several orders of magnitude greater than the actual relaxation time. This would mean that the electrical forces acting on the dispersed phase droplets after break-off from the nozzle for the *n*-decanol experiments were essentially zero. Even if this is the case, it is unlikely to have much effect on the simulated droplet trajectories because even when the relaxation time is around 0.35 s as for the simulations, the buoyancy and drag forces dominate. In this case the solution algorithm reached convergence at this value of relaxation time with further reductions making negligible difference.

For the case of the silicone oil, Fig. 7, the value of relaxation time used in the simulation was 6.2 s. Using the formula for relaxation time ($\tau = \varepsilon\varepsilon_0/K$) and the experimentally determined value of the dielectric constant of silicone oil ($\varepsilon = 2.63$), the corresponding conductivity value is $3.8 \times 10^{-12}\,\mathrm{S\,m^{-1}}$.

Wu and Conrad [10] measured the conductivity of silicone oil as a function of water content. They found that the conductivity at 22 °C varied from about $8 \times 10^{-14}\,\mathrm{S\,m^{-1}}$ at low water content to about $8 \times 10^{-12}\,\mathrm{S\,m^{-1}}$ at the highest water content. The calculated value of conductivity, $K = 3.8 \times 10^{-12}\,\mathrm{S\,m^{-1}}$, is well within the range determined by Wu and Conrad [10] and is near to the high water content value of conductivity ($8 \times 10^{-12}\,\mathrm{S\,m^{-1}}$). This would be consistent with the fact that the silicone oil was equilibrated with water prior to the experiments. This therefore gives credence to the adjustment of the relaxation time to produce a best fit between the experimental and simulated trajectories.

The trajectory data in Fig. 7 clearly show the drop repulsion which occurs when descending water drops reach the vicinity of the lower electrode and experience repulsive forces and thus move back up the column. The data for the drops in Fig. 7 indicate an approximate descent time of 2 s, followed by a short period of movement in an upward direction. The likely explanation for the drop repulsion is that drops acquire dipolar charge as they move in the electric field resulting in charge–charge repulsion as the drop approaches the lower electrode. This cyclic charge polarisation and resultant flow reversal is well documented for charged particles in an electrical field in a gas [11]. The simulation scheme handles this very well and gives an accurate prediction as shown in Fig. 7. The same effect was not observed in the case of either the sunflower oil or the decanol systems. The likely explanation is that silicone oil has a much higher relaxation time (lower conductivity) than either sunflower oil or *n*-decanol and thus the droplets would retain a greater proportion of their initial charge as they travel down the column.

5. Conclusions

A reliable and accurate experimental technique for the recording of the three-dimensional trajectories of charged drops in a liquid–liquid contactor has been demonstrated in this study. The use of image analysis software for the interrogation of the motion of small drops in complex motion has also been demonstrated.

A robust and accurate simulation scheme based on a fundamental approach to charged drop motion in a non-linear electrical field has been demonstrated for the prediction of one-dimensional drop motion. The ability of the scheme to predict reverse droplet flow to due to charge induced repulsion is particularly noteworthy. The scheme has been shown to work well for a range of liquid mixtures, in contactors of two different sizes, and at two different flowrates.

The results give confidence that charged drop motion in three dimensions will be accurately predicted.

References

[1] H.R.C. Pratt, G.W. Stevens, in: J.D. Thornton (Ed.), Science and Practice of Liquid–Liquid Extraction, Clarendon Press, Oxford, 1992, pp. 492–591.
[2] O. Levenspiel, Chemical Reaction Engineering, third ed., Wiley, New York, 1998.
[3] P.J. Bailes, J.D. Thornton, in: Proceedings of the International Solvent Extraction Conference, SCI London, vol. 2, 1971, pp. 1431–1439.
[4] G.J. Laughland, M.K. Millar, L.R. Weatherley, in: J.D. Thornton, W. Batey (Eds.), Proceedings of the Extraction'87, IChemE Symposium Series No. 103, 1987, pp. 263–279.
[5] J. Petera, D. Rooney, L.R. Weatherley, Chem. Eng. Sci. 53 (1998) 3781–3792.
[6] L.A. Bozzi, J.Q. Feng, T.C. Scott, A.J. Pearlstein, J. Fluid Mech. 336 (1997) 1–32.
[7] J. Petera, L.R. Weatherley, Chem. Eng. Sci. 56 (2001) 4929–4947.
[8] L.R. Weatherley, Heat Recov. Syst. CHP 13 (1993) 515–537.
[9] A.P. Hume, M.E. Thesis, University of Canterbury, New Zealand, January 2002.
[10] C.W. Wu, H. Conrad, J. Phys. D: Appl. Phys. 31 (23) (1998) 3403–3409.
[11] J. Cross, Electrostatics: Principles, Problems and Applications, Adam Hilger, Bristol, 1987.